JOURNAL OF GEOPHYSICAL RESEARCH, VOL. 106, NO. D24, PAGES 33,605–33,621, DECEMBER 27, 2001

Carbon and energy exchange by a black spruce-moss ecosystem under changing climate: Testing the mathematical model *ecosys* with data from the BOREAS experiment

R. F. Grant
Department of Renewable Resources, University of Alberta, Edmonton, Alberta, Canada

M.L. Goulden
Department of Earth System Science, University of California, Irvine, California, U.S.A.

S.C. Wofsy
Department of Earth and Planetary Sciences, Harvard University, Cambridge, Massachusetts, U.S.A.

J.A. Berry
Department of Plant Biology, Carnegie Institution of Washington, Stanford, California, U.S.A.

Abstract. There is some uncertainty whether net ecosystem productivity (NEP) of boreal black spruce forests is positive or negative under current climates and how NEP would change under hypothesized changes in future climates. The mathematical model *ecosys* was used to examine NEP of a boreal black spruce forest by testing rates of C transfer simulated from an integrated set of scientific hypotheses against rates measured with chamber, micrometeorological, isotopic and allometric techniques at the northern old black spruce site of the Boreal Ecosystem-Atmosphere Study (BOREAS). Daily aggregations of modeled and measured hourly C fluxes indicated that NEP rose with solar radiation if air temperatures remained below 15°C, but declined if air temperatures rose above 20°C. Daily NEP was thus largest under the higher radiation and lower temperatures of June, but declined under the lower radiation and higher temperatures of July and August. Yearly aggregations of modeled hourly C fluxes indicated that under current (1994–1996) climate NEP of the 150 year old northern old black spruce site was about 40 (wood) + 15 (soil) = 55 g C m^{-2} yr^{-1}. Moss was estimated to contribute about 0.25 of net primary productivity (NPP) at this site and was thus an important component of ecosystem C exchange. The model was then used to predict changes in NEP at the old northern old black spruce site under the IS92a climate change scenario. After 150 years NEP was predicted to be 120 (wood) minus 10 (soil) = 110 g C m^{-2} yr^{-1}. Cumulative gains of C under this scenario were predicted to be 5700 (wood) minus 700 (soil) = 5000 g C m^{-2} after 150 years. Gains of wood C would be vulnerable to loss by fire and insects, both of which could also increase under warmer climates.

1. Introduction

Boreal coniferous forests may have an important effect on global C balances because of their vast area and large C reserves. Several climate change predictions indicate that warming will be most rapid in the continental regions of the boreal zone and so there is great concern about how the net C storage of these forests will be affected by rising temperatures and atmospheric CO_2 concentrations (C_a). Boreal coniferous forests are currently thought to be sinks for atmospheric CO_2 [*Sellers et al.*, 1997] based on seasonal variation and isotopic analyses of C_a [e.g. *Ciais et al.*, 1995; *Keeling et al.*, 1995]. However climate effects on C storage are the net result of those on gross primary productivity (GPP) and autotrophic respiration (R_a) of both overstory and understory, and on heterotrophic respiration (R_h) of the forest floor and the soil. The effects of climate on each of these fluxes differ such that the dependence of C storage on climate may be complex and difficult to predict.

Goulden et al. [1997] reported that GPP of a black spruce – moss forest in northern Manitoba increased with photosynthetic photon flux density (PPFD) up to 500–700 μmol m^{-2} s^{-1} and with air temperature up to 14°C. A strong stomatal constraint to GPP in this forest type was apparent from midday evaporative fractions (LE/R_n) of only 0.35 to 0.45 measured by *Jarvis et al.* [1997] and *Pattey et al.* [1997] in central Saskatchewan. This constraint was also apparent in the low stomatal conductances of black spruce needles (0.025 to 0.035 mol m^{-2} s^{-1}) measured by *Middleton et al.* [1997] and has been associated with low foliar N concentrations rather than low soil water potentials. *Goulden et al.* [1997] reported that respiration of a black spruce – moss forest increased exponentially with temperature, suggesting that rising temperatures could cause smaller increases in GPP than in R_a and R_h that would, beyond a certain point, cause net ecosystem productivity (NEP = GPP – R_a – R_h) to decline.

Paper number 2001JD900064.
0148-0227/01/2001JD900064$09.00

The complexity with which C storage depends on climate has led to the use of process-based ecosystem models to examine NEP under current climates and to predict NEP under hypothesized climates. The improvement of these models is a key objective of the Boreal Ecosystem-Atmosphere Study (BOREAS) which is to be achieved by collecting data for mass and energy exchange at temporal and spatial scales appropriate to well constrained model tests [*Sellers et al.*, 1997]. If these tests are successful under current climates, then the confidence with which such models may be used to predict changes in mass and energy exchange under hypothesized climates would be greatly enhanced.

One ecosystem model included in these tests is *ecosys* [*Grant*, 1996a, 1996b], output from which has been compared with measurements of diurnal mass and energy exchange and of long term C accumulation in a mixed aspen – hazelnut forest [*Grant et al.*, 1999a] and a spruce – moss forest [*Grant et al.*, 2001] in the southern study area of BOREAS. This model simulates hourly GPP, R_a and R_h as affected by soil and plant temperatures [*Grant*, 1993a, 1994b; *Grant et al.*, 1993a, 1993b; *Grant and Rochette*, 1994; *Grant et al.*, 1995b], soil and plant water contents [*Grant et al.*, 1993a, 1993b; *Grant and Rochette*, 1994], soil and plant N and P concentrations [*Grant*, 1991, 1998a; *Grant and Robertson*, 1997], soil and plant aeration [*Grant*, 1993b, 1995; *Grant et al.*, 1993c, 1993d; *Grant and Pattey*, 1999], and by C_a [*Grant et al.*, 1995a, 1995c, 1999b], air temperature and irradiance [*Grant*, 1992a, 1992b; *Grant et al.*, 1999a].

In this study *ecosys* was used to study climate effects on NEP in a boreal coniferous forest by comparing hourly model output for C and energy exchange under changing weather conditions with eddy correlation fluxes measured by *Goulden et al.* [1997] over a 150 year old black spruce – moss forest in northern Manitoba. These ecosystem scale tests were supported by smaller-scale comparisons of C fluxes modeled over the moss surface with fluxes measured in automated chambers by *Goulden and Crill* [1997], and of CO_2 fixation rates modeled at needle surfaces with fixation rates measured in climate - controlled leaf chambers by *Berry et al.* [1998]. These model tests extend those conducted by *Amthor et al.* [this issue] as part of an intercomparison of nine ecosystem models. *Ecosys* was then used to predict NEP of a black spruce – moss forest in northern Manitoba during the next 150 years under an IS92a climate change scenario.

2. Model Development

A detailed description of the algorithms on which *ecosys* is based, and of the testing to which they have been subjected, is given in Grant, 2001. A general description of those parts of the model most relevant to the study reported here is given below. A summary description of *ecosys* and other ecosystem models is given in *Amthor et al.* [this issue].

2.1. Net Primary Productivity

2.1.1. CO_2 Fixation. CO_2 fixation is calculated in *ecosys* from coupled algorithms for carboxylation and diffusion. Carboxylation rates are calculated for each leaf surface of multispecific plant canopies, defined by height, azimuth, inclination and exposure (sunlit versus shaded), as the lesser of dark and light reaction rates [*Grant et al.*, 1999b] according to *Farquhar et al.* [1980]. These rates are driven by irradiance (rectangular hyperbola), temperature (Arrhenius kinetics) and CO_2 concentration (Michaelis-Menten function). Maximum dark or light reaction rates used in these functions are determined by specific activities and surficial concentrations of rubisco or chlorophyll respectively. These activities and concentrations are determined by environmental conditions during leaf growth (CO_2 fixation, water, N and P uptake) as described in section 2.1.4.

Diffusion rates are calculated for each leaf surface from the CO_2 concentration difference between the canopy atmosphere and the mesophyll multiplied by leaf stomatal conductance [*Grant et al.*, 1999b] required to maintain a set C_i: C_a ratio at the leaf carboxylation rate. Stomatal conductance is also an exponential function of canopy turgor generated from a convergence solution for canopy water potential at which the difference between transpiration and root water uptake equals the difference between canopy water contents at the water potentials of the previous and current time steps [*Grant et al.*, 1999b]. Canopy transpiration is solved from a first order solution to the canopy energy balance [*Grant et al.*, 1999b].

2.1.2. Autotrophic Respiration and Senescence. The product of CO_2 fixation is added to a pool of stored C for each branch (defined here as a complete subcomponent of a plant including twigs and foliage) of each plant species from which C is oxidized to meet maintenance respiration requirements using a first order function of stored C [*Grant et al.*, 1999b]. If the pool of stored C is depleted, the C oxidation rate may be less than the maintenance respiration requirement, in which case the difference is made up through respiration of remobilizable C in leaves and twigs. Upon exhaustion of the remobilizable C in each leaf and twig, the remaining C is dropped from the branch as litterfall and added to residue at the soil surface where it undergoes decomposition as described in section 2.2. Environmental constraints such as nutrient, heat or water stress which reduce net C fixation and hence C storage will therefore accelerate litterfall. When oxidation of stored C exceeds maintenance respiration, the excess is used for growth respiration to drive the formation of new biomass [*Grant et al.*, 1999b] as described in section 2.1.4.

2.1.3. Nutrient Uptake. Nutrient (N and P) uptake is calculated for each plant species by solving for aqueous concentrations of NH_4^+, NO_3^- and $H_2PO_4^-$ at root and mycorrhizal surfaces in each soil layer at which radial transport by mass flow and diffusion from the soil solution to the surfaces equals active uptake by the surfaces [*Grant and Robertson*, 1997; *Grant*, 1998b]. This solution dynamically links rates of soil nutrient transformations with those of root and mycorrhizal nutrient uptake. Nutrient transformations control the aqueous concentrations of NH_4^+, NO_3^- and $H_2PO_4^-$ in each soil layer through thermodynamically driven precipitation, adsorption and ion pairing reactions [*Grant and Heaney*, 1997], convective-dispersive solute transport [*Grant and Heaney*, 1997], and microbial mineralization-immobilization [*Grant et al.*, 1993a]. Active uptake is calculated from length densities and surface areas [*Itoh and Barber*, 1983] given by a root and mycorrhizal growth submodel [*Grant*, 1993a, 1993b, *Grant*, 1998b; *Grant and Robertson*, 1997]. Active nutrient uptake is constrained by O_2 uptake [*Grant*, 1993a,b], by solution NH_4^+, NO_3^- and $H_2PO_4^-$ concentrations, and by concentrations of C , N and P stored by root and mycorrhizae [*Grant*, 1998b]. The products of N and P uptake are stored in root and mycorrhizal pools from which they are combined with stored C when driven by growth respiration to form new plant biomass as described in section 2.1.4. Plant species designated as legumes in the model also grow

root nodules in which aqueous N_2 is reduced to stored N through oxidation of stored C according to the energetics of *Schubert* [1982]. This reduction generates concentration gradients of stored C, N and P between nodule and root that drives nutrient exchange.

2.1.4. Plant Growth. Growth respiration from section 2.1.2 drives expansive growth of vegetative and reproductive organs through mobilization of stored C, N and P in each branch of each plant species according to phenology-dependent partitioning coefficients and biochemically based growth yields. This growth is used to simulate the lengths, areas and volumes of individual internodes, twigs and leaves [*Grant,* 1994b; *Grant and Hesketh,* 1992] from which heights and areas of leaf and stem surfaces are calculated for irradiance interception and aerodynamic conductance algorithms used in energy balance calculations. Growth respiration also drives extension of primary and secondary root axes and of mycorrhizal axes of each plant species in each soil layer through mobilization of stored C, N and P in each root zone of each plant species [*Grant,* 1993a, 1993b, Grant, 1998b]. This growth is used to calculate lengths and areas of root and mycorrhizal axes from which root uptake of water [*Grant et al.,* 1999b] and nutrients [*Grant,* 1991; *Grant and Robertson,* 1997] is calculated.

The growth of different branch organs and root axes in the model depends upon transfers of stored C, N and P among branches, roots and mycorrhizae. These transfers are driven by concentration gradients within the plant which develop from different rates of C, N or P acquisition and consumption by its branches, roots and mycorrhizae [*Grant,* 1998b]. When root N or P uptake rates described in section 2.1.3 are low, stored N or P concentrations in roots and branches become low with respect to those of stored C. Such low ratios in branches reduce the specific activities and surficial concentrations of leaf rubisco and chlorophyll which in turn reduce leaf CO_2 fixation rates. These low ratios also cause smaller root-to-shoot transfers of N and P and larger shoot-to-root transfers of C [*Grant,* 1998b], thereby allowing more plant resources to be directed towards root growth. The consequent increase in root:shoot ratios and thus in N and P uptake, coupled with the decrease in C fixation rate, redresses to some extent the stored C:N:P imbalance when N or P uptake is limiting. The model thus implements the functional equilibrium between roots and shoots proposed by *Thornley* [1995].

2.2. Heterotrophic Respiration

2.2.1. Decomposition. Soil organic matter in *ecosys* is resolved into four substrate-microbe complexes (plant residue, animal manure, particulate organic matter and non-particulate organic matter) within each of which C, N and P may move among five organic states: solid substrate, sorbed substrate, soluble hydrolysis products including acetate, microbial communities, and microbial residues [*Grant,* 1999, Table 1]. Each organic state in each complex is resolved into structural components of differing vulnerability to hydrolysis and into elemental fractions C, N and P within each structural component. Microbial communities are also resolved into functional type including obligate aerobes, facultative anaerobes (denitrifiers), obligate anaerobes (fermenters), methanogens and diazotrophs.

Litterfall from section 2.1.2 is added to the plant residue complex and partitioned into carbohydrate, protein, cellulose and lignin structural components according to *Trofymow et al.* [1995]. Rates of component hydrolysis are the product of the active biomass and specific activity of each microbial functional type within each complex [*Grant et al.,* 1993a; *Grant and Rochette,* 1994]. Specific activity is constrained by substrate-microbe density relationships [*Grant et al.,* 1993a; *Grant and Rochette,* 1994], and by the temperatures and water contents of surface residue and a vertically resolved soil profile [*Grant,* 1997; *Grant and Rochette,* 1994; *Grant et al.,* 1998]. A fraction of the hydrolysis products of lignin is coupled with those of protein and carbohydrate according to the stoichiometry proposed by *Shulten and Schnitzer* [1997] and the resulting compound is transferred to the solid substrate of the particulate organic matter complex. Rates of particulate organic matter formation are thus determined by substrate lignin content and heterotrophic microbial activity.

2.2.2. Microbial Growth. The concentration of the soluble hydrolysis products in section 2.2.1 determines rates of C oxidation by each heterotrophic population, the total of which drives CO_2 emission from the soil surface. This oxidation is coupled to the reduction of O_2 by all aerobic populations [*Grant et al.,* 1993a, 1993b; Grant and Rochette, 1994], to the sequential reduction of NO_3^-, NO_2^- and N_2O by heterotrophic denitrifiers [*Grant et al.,* 1993c,d; Grant and Pattey, 1999] and to the reduction of organic C by fermenters and of acetate by heterotrophic methanogens [*Grant,* 1998a]. The energetics of these oxidation-reduction reactions determine growth yields and hence the active biomass of each heterotrophic functional type from which its decomposer activity is calculated as described in section 2.2.1. In addition, autotrophic nitrifiers conduct NH_4^+ and NO_2^- oxidation [*Grant,* 1994a] and N_2O evolution [*Grant,* 1995], and autotrophic methanotrophs conduct CH_4 oxidation [*Grant,* 1999], the energetics of which determine autotrophic growth yields and hence biomass and activity. Each microbial population in the model seeks to maintain steady-state ratios of biomass C:N:P by mineralizing or immobilizing NH_4^+, NO_3^- and $H_2PO_4^-$, thereby regulating solution concentrations that drive N and P uptake by roots and mycorrhizae as described in section 2.1.3. Microbial populations undergo first order decomposition, products of which are partitioned between microbial residues within the same substrate-microbe complex, and the solid substrate of the nonparticulate organic matter complex according to soil clay content [*Grant et al.,* 1993a, 1993b]. Rates of nonparticulate organic matter formation are thus determined by rates of microbial decay and by soil clay content.

3. Field Experiment

3.1. Site Description

The old black spruce site in the northern study area of BOREAS (55.9 °N, 98.4 °W) is almost flat, poorly drained, and covered by a dominant canopy of black spruce (*Picea mariana* (Mill.) BSP), average age 155 years, height 9.1 m, density 5450 ha^{-1} from Gower et al., 1997] with a minor shrub layer and feather moss (*Pleurozium schreberi* and *Hylocomium splendens*) in upper locations, and continuous sphagnum moss (*Sphagnum* spp.) in lower locations. The soils at this site range from Eluviated Eutric Brunisols to Gleyed Cumulic and Cumic Humic Regosols. These soils have a 0.1 – 1.6 m peat layer overlying a coarse-textured mineral soil (Table 1).

3.2. Leaf CO_2 Fixation

On August 5 and 6 1996, selected needle clusters near the top of the black spruce canopy were enclosed in the cuvette of a portable gas exchange system (model MPH-1000, Campbell Scientific, Logan Utah) with an infrared gas analyzer (model

Table 1. Physical and Biological Properties of the Cumic Humic Regosol at the Northern Old Black Spruce Site

Depth (m)	.01	.05	.15	.30	.35	.47	.72	.96	1.20
BD (Mg m^{-3})	0.10	0.10	0.10	0.10	1.25	1.52	1.66	1.66	1.66
$\theta_{-.01MPa}$ (m^3 m^{-3})	0.40	0.40	0.40	0.40	.218	.213	.183	.022	.034
$\theta_{-1.5MPa}$ (m^3 m^{-3})	0.20	0.20	0.20	0.20	.056	.049	.050	.012	.013
Sand (kg kg^{-1})					756	728	646	960	949
Silt (kg kg^{-1})					200	214	287	19	30
pH	3.4	3.4	3.4	3.4	4.3	4.3	4.9	5.8	6.6
CEC (cmol kg^{-1})	75.8	75.8	75.8	75.8	9.0	10.1	8.2	2.9	2.5
Org. C (g kg^{-1})	434	434	434	434	11.4	9.8	3.6	1.0	0.5
Org. N (mg kg^{-1})	8162	8162	8162	8162	603	423	215	52	52
Org. P (mg kg^{-1})	900	900	900	900	75	53	27	7	7
Al-P (mg kg^{-1})	0	0	0	0	164	225	192	149	183
Ca-P (mg kg^{-1})	0	0	0	0	0	0	100	150	200

abbreviations: BD, bulk density; θ, water content; CEC, cation exchange capacity; Al-P, aluminium phosphate, calculated from total P – organic P and modeled as variscite; Ca-P, calcium phosphate, calculated from total P – organic P and modeled as hydroxyapatite.

6262, LiCor Inc., Lincoln Nebraska) and a dew point hygrometer (model Dew-10, General Eastern, Woburn, Massachusetts) that enabled precise control of CO_2, temperature, irradiance and humidity at the leaf surface. The leaves were subjected to incremental changes in irradiance or CO_2 with all other environmental conditions held constant. Response of CO_2 flux to increments of ~50 μmol m^{-2} s^{-1} in irradiance was measured at a CO_2 concentration of 360 μmol mol^{-1}, a leaf temperature of 20°C, and a relative humidity of 0.6. Response of CO_2 flux to increments of ~100 μmol mol^{-1} in CO_2 concentration was measured at an irradiance of 2350 μmol m^{-2} s^{-1}, a leaf temperature of 23.5°C and a relative humidity of 0.5, and again at an irradiance of 650 μmol m^{-2} s^{-1}, a leaf temperature of 20.0°C and a relative humidity of 0.3. Measurements of CO_2 flux and stomatal conductance were taken once steady-state values were achieved (usually 30 min. after conditions were changed). Further details are reported by *Berry et al.* [1998].

3.3. Canopy Mass and Energy Exchange

Fluxes of latent heat, sensible heat, CO_2 and momentum were measured by eddy correlation at a height of 29 m and a frequency of 4 Hz with a three-axis sonic anemometer and temperature sensor (Applied Technologies, Boulder, Colorado), and an infrared gas analyzer (model 6262, Li-Cor Inc., Lincoln, Nebraska) following *Wofsy et al.* [1993] and *Goulden et al.* [1996]. CO_2 and water vapor concentrations measured every 12 min at heights of 0.3, 1.5, 4.6, 8.4, 12.9 and 28.8 m were used to calculate hourly changes in canopy CO_2 storage which were added to fluxes measured by eddy correlation to estimate hourly net ecosystem productivity. Soil temperatures were measured with precision thermistors at 0.05, 0.10, 0.20, 0.50 and 1.00 m beneath the moss surface at five sites along a topographic gradient. Details of measurement apparatus, techniques and results are given by *Goulden et al.* [1997].

3.4. CO_2 Exchange Over Moss

An automated gas exchange system sampled air drawn via distribution manifolds through clear 0.38 x 0.385 x 0.25 m chambers inserted to a depth of 0.10 – 0.15 m below the moss surface. Gas samples were taken during 10 min periods after closure of the chambers. Changes in CO_2 and water vapor concentrations during this period were measured with an infrared gas analyzer (model 6262, Li-Cor Inc., Lincoln, Nebraska) operating in absolute mode. CO_2 fluxes over the moss were estimated by extrapolating changes in CO_2 concentrations measured from 2 to 4 min after closure back to the moment of closure. The chambers were then pneumatically raised to a vertical position until the next sampling period 3 hours later. Each chamber was calibrated daily by adding a known CO_2 flux to the return flow during sampling. Further details of gas exchange measurements over moss are given by *Goulden and Crill* [1997].

4. Model Experiment

4.1. Model Initialization and Run

The ecosystem model *ecosys* was initialized with data for the physical properties of a Cumic Humic Regosol (Table 1), and with values for the biological properties of black spruce and moss (Table 2). These values remained the same as those of aspen and hazelnut used in an earlier study of mass and energy exchange (Grant *et al.*, 1999a, Table 3], except for the following changes:

4.1.1. Spruce. (1) The minimum leaf C:N ratio was raised from 6.67 g g^{-1} for broadleaf plants to 20.0 g g^{-1} (≈ 22.5 mg N g DM^{-1}) for coniferous plants based on foliar N concentrations measured in heavily fertilized black spruce by *Mahendrappa and Solonius* [1982]. Actual C:N ratios rise above this minimum value if stored C:N ratios limit plant growth in the model. (2) The interception fraction (clumping index) was reduced from 0.65 for aspen to 0.50 for spruce based on irradiance interception data from *Chen et al.* [1997]. (3) The value of the parameter relating leaf area expansion to leaf mass growth [*Grant and Hesketh*, 1992, equation (4)] was reduced from that used for deciduous plants based on specific leaf areas measured by *Middleton et al.* [1997]. (4) Reflection and transmission coefficients for shortwave radiation were reduced from 0.225 for deciduous leaves to 0.15 for coniferous leaves based on data from *Betts and Ball* [1997]. Reflection and transmission coefficients for photosynthetically active radiation (0.075) were not changed. (5) A model switch used in deciduous trees to force the withdrawal and storage of leaf C, N and P after a cold requirement under shortening photoperiods, and the remobilization of stored nutrients following a heat requirement under lengthening photoperiods was disabled for coniferous trees. (6) Protein, carbohydrate, cellulose and lignin contents of coniferous litter were changed from those of deciduous litter according to *Trofymow et al.* [1995] (Table 1).

Table 2. Key Biological Properties of Spruce, Moss and Soil Microbial Populations Used in *Ecosys*

Variable	Value	Units
	Spruce and Moss	
Maximum carboxylation rate	50	μmol CO_2 g^{-1} rubisco s^{-1} at 30 °C
Maximum rubisco oxygenation rate	10.5	μmol O_2 g^{-1} rubisco s^{-1} at 30 °C
Maximum electron transport rate	500	μmol e^- g^{-1} chlorophyll s^{-1} at 30 °
Quantum efficiency	0.5	μmol e^- μmol quanta
K_m for carboxylation	12.5	μM CO_2 at 30 °C
K_m for oxygenation	500	μM O_2
Transmission & reflection of shortwave radiation	0.15	
Transmission & reflection of PAR	0.075	
Fraction of leaf protein in rubisco	0.10 (spruce) 0.25 (moss)	g (C) g^{-1} (C)
Fraction of leaf protein in chlorophyll	0.02 (spruce) 0.05 (moss)	g (C) g^{-1} (C)
Minimum C:N ratio in leaf	20.0 (spruce) 6.67 (moss)	g (N) g^{-1} (C)
C:N ratio in twig and root	40.0	g (N) g^{-1} (C)
C:N ratio in stem	267	g (N) g^{-1} (C)
Maximum C:P ratio in leaf	200 (spruce) 66.7 (moss)	g (P) g^{-1} (C)
C:P ratio in twig and root	400	g (P) g^{-1} (C)
C:P ratio in stem	2667	g (P) g^{-1} (C)
Maintenance respiration of plant	0.016	g (C) g^{-1} (N) h^{-1} at 30 °C
Growth yield of leaf and twig	0.64	g (C) g^{-1} (C)
Growth yield of stem	0 76	g (C) g^{-1} (C)
Growth yield of root	0.64	g (C) g^{-1} (C)
Interception fraction (spruce)	0.5	m^2 m^{-2}
Interception fraction (moss)	1.0	m^2 m^{-2}
C_i:C_a ratio at non-limiting water	0.7	
Maximum root NH_4^+ uptake rate	0.025	g (N) m^{-2} root area h^{-1} at 30 °C
K_m for root NH_4^+ uptake	0.40	g (N) m^{-3}
Minimum NH_4^+ conc'n for root uptake	0 03	g (N) m^{-3}
Maximum root PO_4^{2-} uptake rate	0.005	g (P) m^{-2} root area h^{-1} at 30 °C
K_m for root PO_4^{2-} uptake	0.075	g (P) m^{-3}
Minimum PO_4^{2-} conc'n for root uptake	0.002	g (P) m^{-3}
	Soil	
Litterfall protein content	0 07 (spruce) 0.07 (moss)	g (C) g^{-1} (C)
Litterfall carbohydrate content	0.27 (spruce) 0 34 (moss)	g (C) g^{-1} (C)
Litterfall cellolose content	0 36 (spruce) 0.43 (moss)	g (C) g^{-1} (C)
Litterfall lignin content	0.30 (spruce) 0.16 (moss)	g (C) g^{-1} (C)
Specific activity of protein decomposition	1.0	g (C) g^{-1} micr. (C) h^{-1} at 30 °C
Specific activity of carbohydrate decomposition	1.0	g (C) g^{-1} micr. (C) h^{-1} at 30 °C
Specific activity of cellulose decomposition	0.15	g (C) g^{-1} micr. (C) h^{-1} at 30 °C
Specific activity of lignin decomposition	0.025	g (C) g^{-1} micr. (C) h^{-1} at 30 °C
Specific activity of active OM decomposition	0.025	g (C) g^{-1} micr. (C) h^{-1} at 30 °C
Specific activity of humus decomposition	0.005	g (C) g^{-1} micr (C) h^{-1} at 30 °C
Specific respiration rate	0.20	g (C) g^{-1} micr. (C) h^{-1} at 30 °C
K_m for microbial C uptake	35	g (C) m^{-3}
Maintenance resp'n of labile biomass	0.010	g (C) g^{-1} micr. (N) h^{-1} at 30 °C
Maintenance resp'n of resistant biomass	0.0015	g (C) g^{-1} micr. (N) h^{-1} at 30 °C
Energy yield of C oxid'n with O_2 reduction	37.5	kJ g^{-1} (C)
Energy yield of C oxid'n with NO_x reduction	10.0	kJ g^{-1} (C)
Energy yield of C oxid'n with acetate reduction	1.03	kJ g^{-1} (C)
Energy requirement for microbial growth	25.0	kJ g^{-1} (C)
Requirement of C oxidation for N_2 fixation	6.0	g (C) g^{-1} (N)

4.1.2. Moss. (1) The shape parameter relating leaf turgor to stomatal resistance used for vascular plants [*Grant et al.*, 1999b, equation (13)] was set to zero for moss, thereby replacing the dynamic stomatal response to turgor with a constant diffusive resistance taken from *Proctor* [1982]. This constant resistance forced moss water potential to equilibrate with atmospheric relative humidity during the convergence solution for energy exchange. (2) The effect of plant water status on CO_2 fixation in moss was calculated from the relative humidity associated with moss water potential according to data given by *Proctor* [1982] and in *Clymo and Hayward* [1982], rather than from stomatal resistance and water potential as in vascular plants.

All other model parameters for C fixation, respiration and partitioning by plant and microbial populations were the same as those used in earlier studies of C and energy exchange over agricultural crops [*Grant and Baldocchi*, 1992; *Grant et al.*, 1993e, 1995c], forests [*Grant et al.*, 1999a] and soils [*Grant*, 1994a, 1997; Grant and Rochette, 1994; Grant et al., 1993a,

Table 3. Annual Carbon Balance of a 150 Year Old Black Spruce - Moss Forest in Northern Manitoba Estimated From Flux Measurements and Allometric Techniques During 1994, and Simulated by *Ecosys* Under 1994, 1995 And 1996 Climate and Under 1996 Climate After 150 Years of IS92a Climate Change

	Estimated (g C m^{-2})	Simulated (g C m^{-2})			
	1994	1994	1995	1996	IS92a
		Spruce			
Gross primary productivity		624	600	574	716
Autotrophic respiration[a]		396	366	368	469
Net primary productivity		228	234	206	247
Senescence	46[d] + 90[e]	179	171	141	101
Exudation		26	19	19	21
Net Growth	20[i],78[d]	23	44	46	125
		Moss			
Gross primary productivity		179	180	201	282
Autotrophic respiration[a]		108	104	121	175
Net primary productivity	50 – 150[g]	71	76	80	107
Senescence		72	76	75	107
Exudation		1	2	3	3
Net growth	12[d]	-2	-3	4	-4
Change in storage		1	1	-2	1
		Soil			
Heterotrophic respiration[b,c]		245	243	226	242
		Ecosystem			
Gross primary productivity	800[h],1080[f]	803	780	775	998
Total respiration	800[h]	749	713	715	886
Net ecosystem productivity	-40[j]	54	67	60	112
Net primary productivity	219[d,e],252[f]	299	310	286	354
Change in plant C		21	43	50	122
Change in soil C	10 – 30[g],-80[j]	33	24	10	-10

[a] Includes root respiration [b] Excludes root respiration [c] Includes CO_2-C and CH_4-C [d] Gower et al. (1997) above-ground [e] Steele et al. (1997) below-ground [f] Ryan et al. (1997) [g] Harden et al. (1997) [h] Goulden et al. (1997) [i] Alberta Forest Service (1985) [j] Goulden et al. (1998)

1993b, 1993c, 1993d, 1995b, 1998]. The values of all model parameters were derived independently of data recorded at the field site.

The lower boundary of the modeled soil profile was set to prevent subsurface drainage or capillary rise. The upper boundary of the modeled soil profile was set to allow fairly rapid surface runoff so that any water accumulating beyond the surface storage capacity of the soil was removed within a few hours. These settings were intended to simulate the hydrology of the field site which had poor subsurface drainage but fairly good surface drainage. The model was then run for 150 years under random yearly sequences of hourly averaged meteorological data (air temperature, humidity and wind speed) recorded at the flux tower during 1994, 1995 and 1996 [*Sutton et al.*, 1998], supplemented with 1 km^2 gridded data (shortwave radiation and precipitation) generated from surface measurements. Model C_a was initialized at 280 μmol mol^{-1} and incremented daily at a rate of 0.00167 yr^{-1} so that C_a recorded in 1996 would be reached after 150 years. Atmospheric N deposition in the model occurred as NO_3^- dissolved in precipitation (0.5 g N m^{-3}) and as NH_4^+ from adsorption of atmospheric NH_3 (0.004 μmol mol^{-1}) by leaves and soil surfaces. During the first year of the run, spruce and moss were seeded onto the forest floor at 0.6 m^{-2} [*Gower et al.*, 1997] and 10^4 m^{-2} [*Clymo and Hayward*, 1982] respectively. No other interventions occurred during the entire run.

4.2. Leaf CO_2 Fixation

After completion of the model run, all state variables in the model were initialized with the values they had held at the end of August 5 in the 150th year of the model run during which 1996 meteorological data had been used. The model was then run for 24 hours under incremental changes in irradiance or C_a with all other environmental conditions maintained at values used in the leaf CO_2 fixation study described in section 3. Steady state values for net CO_2 fixation rates (CO_2 fixation – maintenance respiration from Table 2) and stomatal conductances were attained within 12 hourly time steps of the start of each model run. Fixation rates and conductances simulated for an individual leaf surface in the upper part of the spruce canopy were compared with measured values. Because conifer needle surfaces used in the CO_2 fixation study were assumed to be randomly oriented towards incident irradiance, simulated values were taken as the average of those for all leaf orientation classes (azimuth and inclination as described in section 2.1.1) represented in the model.

4.3. Canopy Mass and Energy Exchange

During the same year of the model run as that used in the leaf CO_2 fixation study described above, hourly mass and energy exchange over the spruce-moss stand simulated under 1996 meteorological data were compared with results obtained from

the flux tower at the field site during 1996. Simulated CO_2 and energy fluxes over the spruce were calculated as the sum of those from the soil surface, the surface detritus, the moss and the spruce. Simulated CO_2 and energy fluxes over the moss were calculated as the sum of those from the soil surface, the surface detritus and the moss. Soil temperatures simulated in the midpoint of the detritus layer beneath the moss, and in the organic layer 0.10 m below the midpoint of the detritus layer, were compared with those measured 0.10 and 0.20 m below the surface of the moss. Three one week periods were selected for comparison during 1996. The first was in late spring (June 18-24) to observe model behavior during a transition from clear warm weather to cool cloudy weather. The second was in mid summer (July 25-31) to observe model behavior during a period of clear weather with rising temperatures. The third was in late summer (August 30 to September 5) to observe model behavior when the weather was cooling.

4.4. Long-Term C Exchange

Model results for annual net primary productivity (NPP), net ecosystem productivity (NEP) and aboveground phytomass growth of a 150 year old spruce-moss forest under 1994 climate were then compared with estimates of NPP, NEP and growth derived from aggregated flux data, tree ring analyses and other measurements taken at the field site during 1994. Long-term model results for C accumulation in spruce wood and soil were compared with results from measurements of spruce growth and forest floor development in the same ecological zone as that of the field site.

The model run was then extended for another 150 years using the same soil and plant properties, but with changes in atmospheric boundary conditions selected from *Kattenberg et al* [1996]. These changes were applied to the same sequence of hourly-averaged meteorological data used in the first run. A compound increase in C_a of 0.007 yr^{-1} calculated daily was used to simulate a doubling of concentration over 100 years according to the IPCC IS92a emissions scenario. This increase was accompanied by simple daily increases in maximum and minimum air temperature that depended upon time of day and time of year. Maximum daily temperatures rose more slowly (average 0.0275°C yr^{-1}) than did minimum daily temperatures (average 0.0325°C yr^{-1}) in order to simulate a reduction in diurnal temperature ranges caused by increased evaporative cooling and aerosol loading [*Kattenberg et al.*, 1996]. Both maximum and minimum daily temperatures rose more slowly during spring and summer than during autumn and winter [*Kattenberg et al.*, 1996]. Changes in the hourly temperatures used by *ecosys* were interpolated from those in maximum and minimum daily temperatures. These temperature changes resulted in an average cumulative increase of 3.125°C after 100 years which is less than one of 4.5°C under 2 x C_a estimated for western Canada by the Canadian Climate Centre GCM [*Boer et al.*, 1992] but is consistent with one of between 2°C and 3°C estimated under IS92a with aerosol loading by *Mitchell et al.* [1995]. Because relative humidity was unchanged from that in the control run while temperature rose, atmospheric vapor density also rose as is predicted from increased evaporation rates. Simple increases in precipitation of 0.001 yr^{-1} were derived from a number of climate simulations using IS92a presented by *Kattenberg et al.* [1996]. These increases are equivalent to 10% after 100 years which is similar to one of 11% under 2 x C_a estimated for western Canada by the Canadian Climate Centre GCM [*Boer et al.*, 1992]. Solar radiation and wind speed were unchanged from current values. Model results for GPP, NPP, NEP and long-term C accumulation were then compared with those under current climate.

5. Results

5.1. Leaf CO_2 Fixation

Soil C:N ratios of > 50 in the organic layer of the northern old black spruce site (Table 2) limited N mineralization in the model, causing soil mineral N to remain at extremely low concentrations (< 0.2 g NO_3^- N m^{-3}) during the model run. Large soil C:N ratios are characteristic of boreal coniferous sites [e.g. *Mugasha et al.*, 1991] and are more than double those required for rapid mineralization and uptake of N in forest soils [*Troth et al.*, 1976]. Under these conditions rates of N uptake by root and mycorrhizal surfaces in the model (from parameters in Table 1) were constrained by those of net N mineralization from microbial activity. This constraint on uptake caused large stored C:N ratios to develop in the spruce and moss, which in turn caused leaf C:N ratios in the model to rise from set minimum values given in Table 1. These values resulted in areal N densities in the current year's foliage of 1.5 g N m^{-2}, which was at the upper end of the range of areal N densities measured at the old black spruce site by *Dang et al.* [1997].

These activities and densities determined the modeled responses of needle CO_2 fixation to irradiance and C_a shown in Figure 1. The slope of the irradiance response curve at low irradiance (Figure 1a) was determined by the chlorophyll activities and densities, and by the quantum and carboxylation efficiencies used to calculate light reaction rates in the model for which theoretical maxima were used (Table 1). The transition to irradiance-saturated CO_2 fixation at higher irradiance was determined by the specific activities and densities of rubisco used to calculate dark reaction rates in the model (Table 1), and by the shape parameter used in the irradiance response function. This transition occurred in the model at an irradiance of ~300 μmol m^{-2} s^{-1}, whereas the measured data indicated a more gradual transition at ~200 μmol m^{-2} s^{-1}. The response of CO_2 fixation to rising C_a in the model (Figure 1b) was determined by the activities and densities of rubisco at lower C_a and by those of chlorophyll at higher C_a (Table 1). This response was shaped by the relationship between aqueous CO_2 concentration and the K_m for carboxylation (Table 1) as affected by the K_m for oxygenation and by temperature. The modeled response of CO_2 fixation to rising C_a was independent of the irradiance levels tested at low C_a, but was increasingly constrained by irradiance at higher C_a. The measured response was constrained by irradiance at all C_a.

5.2. Diurnal Mass and Energy Exchange

A transition from clear warm weather (> 25°C) to cool cloudy weather (< 10°C) between June 19 and 20 (DOY 171 and 172 in Figure 2a), accompanied by precipitation (Figure 2b) and soil cooling (Figure 2c), was followed by a transition to clear, cool weather on June 22 (DOY 174 in Figure 2a). The presentation of mass and energy fluxes follows the convention that downward fluxes are positive (i.e. gains to the ecosystem) and upward fluxes are negative (i.e. losses to the ecosystem). Both modeled and measured upward latent heat fluxes remained low (< 200 W m^{-2}) through both transitions (Figure 3a). In the model low latent heat fluxes were attributed to low stomatal conductances caused by low CO_2 fluxes (Figure1) caused in turn

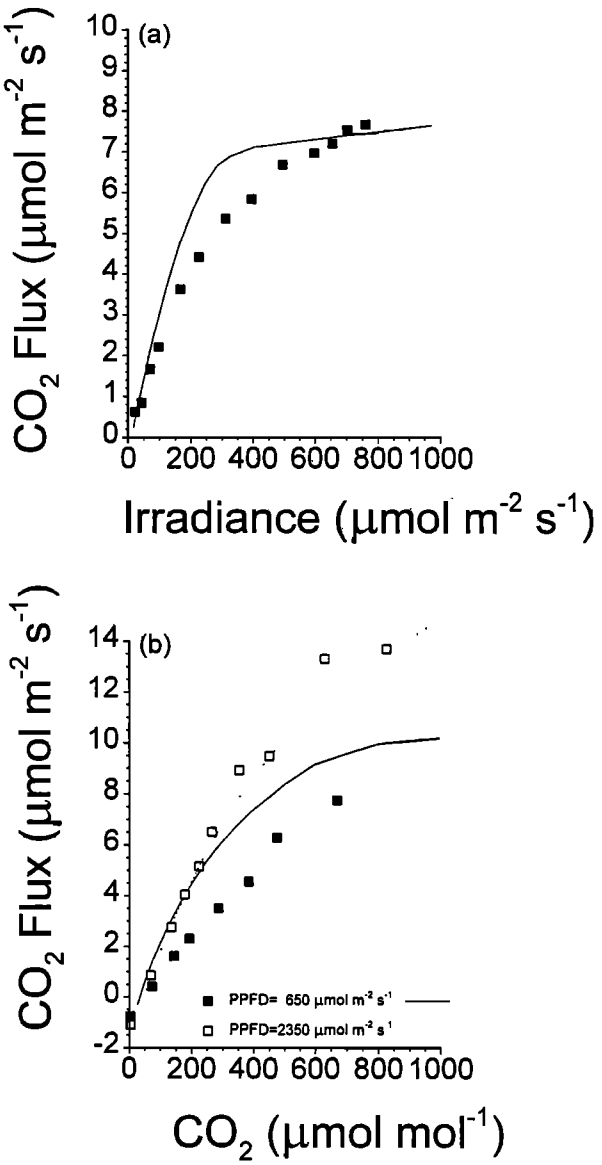

Figure 1. Simulated (lines) and measured (symbols) responses of CO_2 fixation by needles in the upper part of a spruce canopy to changes in (a) irradiance (C_a = 360 μmol mol^{-1}, T_a = 20 °C, H_a = 0.6) and (b) CO_2 concentration (I = 2350 μmol m^{-2} s^{-1}, T_a = 23.5 °C, RH = 0.5, and I = 650 μmol m^{-2} s^{-1}, T_a = 20.0 °C, H_a = 0.3).

by low activities and densities of rubisco and chlorophyll under high C:N ratios. Low stomatal conductances caused changes in net radiation to be offset by changes in sensible heat flux during both weather transitions. Downward sensible heat fluxes simulated during nights with low wind speeds (DOY 172, 173 and 174 in Figure 2b) were not measured (Figure 3a). *Amthor et al.* [this issue] describe the difficulties in measuring C and energy fluxes with eddy correlation under low wind speeds.

The transition from clear warm weather to cool, cloudy weather on June 20 caused both downward (daytime) and upward (nighttime) CO_2 fluxes measured and modeled over the black spruce to decline below 5 μmol m^{-2} s^{-1} (Figure 3b). The transition to cool, clear weather on June 22 caused downward fluxes to rise above 5 μmol m^{-2} s^{-1} while upward fluxes remained below 5 μmol m^{-2} s^{-1}, indicating a rise in daily NEP with high irradiance and cool temperatures. Downward fluxes over spruce in the model were larger than those measured under clear weather during this period. Both downward and upward CO_2 fluxes measured and modeled over the moss were about 2 – 3 μmol m^{-2} s^{-1}.

A continuous warming from below 20°C to above 25°C occurred under clear (Figure 4a), dry (Figure 4b) conditions from July 25 to 31 (DOY 207 to 213). There was some evidence that R_n was underestimated by the model. However the ratio of simulated R_n to total shortwave radiation provided from the gridded dataset was the same as that measured over boreal coniferous forests by *Kaminsky and Dubayah* [1997], suggesting that the radiative transfer algorithms in the model were not in error. This warming caused only a small rise in upward latent heat flux from 150 to 200 W m^{-2} (Figure 5a), indicating continuing stomatal constraints that caused net radiation to be dissipated mostly as sensible heat. Warming of the air (Figure 4a) and soil (Figure 4b) caused downward CO_2 fluxes measured and modeled over the spruce to decline below 5 μmol m^{-2} s^{-1} and upward CO_2 fluxes to rise above 5 μmol m^{-2} s^{-1}, indicating a decline in daily NEP with warming. During this period downward and upward CO_2 fluxes measured and modeled over the moss were comparable, indicating an approximate C balance on a daily basis.

A continuous cooling from above 25°C to below 15°C (Figure 6a) occurred under dry conditions (Figure 6b) between August 30 and September 5 (DOY 243 to 249). Upward latent heat fluxes declined to < 100 W m^{-2} during this period, so that changes in net radiation were almost entirely offset by changes in sensible heat (Figure 7a). Downward CO_2 fluxes remained above 5 μmol m^{-2} s^{-1} while upward CO_2 fluxes declined below 5 μmol m^{-2} s^{-1} (Figure 7b), indicating a rise in daily NEP with cooling. With shortening daylengths in early September, the duration of downward CO_2 fluxes measured and modeled within each day was less than that in June (Figure 3b) and July (Figure 5b). Both downward and upward CO_2 fluxes measured and modeled over moss were about 2 μmol m^{-2} s^{-1} (Figure 7b). Other comparisons of modeled versus measured fluxes of CO_2 and water are given by *Amthor et al.* [this issue].

5.3. Daily C and Water Exchange

Daily totals of NEP measured over spruce during 1996 indicated losses of 0.3 to 0.6 g C m^{-2} d^{-1} until mid-May followed by gains that rose to 2 – 3 g C m^{-2} d^{-1} by late June, after which gains declined to near zero by late September (Figure 8a). Modeled NEP followed the same trend, although peak rates during late May and early June were higher than those measured by about 1 g C m^{-2} d^{-1}. Both modeled and measured NEP showed large day-to-day variation. In the model, much of this variation was attributed to short-term changes in weather. The rapid transition from negative NEP on DOY 172 and 173 to large positive NEP on days 174 and 175 (Figure 8a) was attributed to a rise in radiation without a rise in air and soil temperature (Figure 2a,c) that raised GPP without raising R_a and R_h (Figure 3b). The transition from positive to negative NEP between DOY 206 and 213 (Figure 8) was attributed to rising air and soil temperatures (Figure 4a,c) that raised R_a and R_h more than GPP (Figure 5b). The transition from negative to positive NEP between DOY 242 and 248 (Figure 8) was attributed to declining air and soil temperatures (Figure 6a,c) that reduced R_a and R_h more than GPP (Figure 7b). The relationship between daily NEP measured and modeled during 1996 is shown in Figure 8b. A statistical

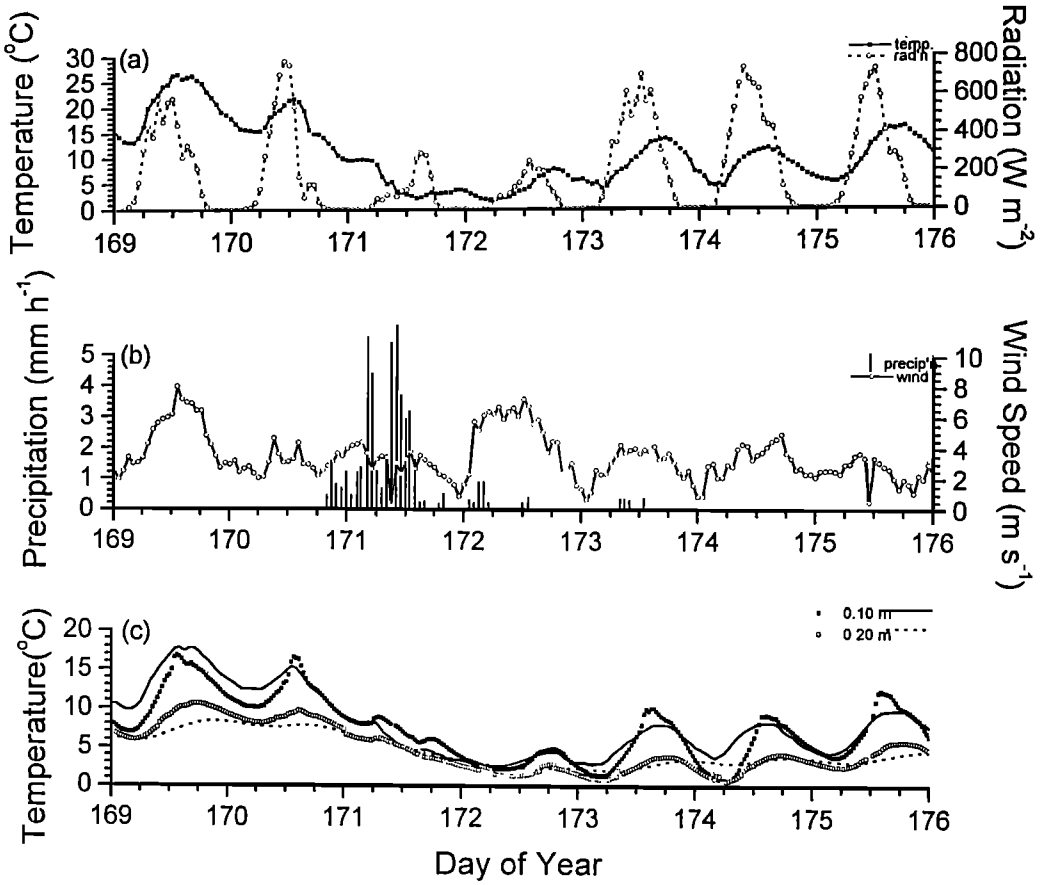

Figure 2. (a) Air temperature, radiation (b) precipitation, wind speed and (c) soil temperatures simulated (lines) and measured (symbols) at the northern old black spruce site from June 18 to 24 (DOY 170 to 176), 1996.

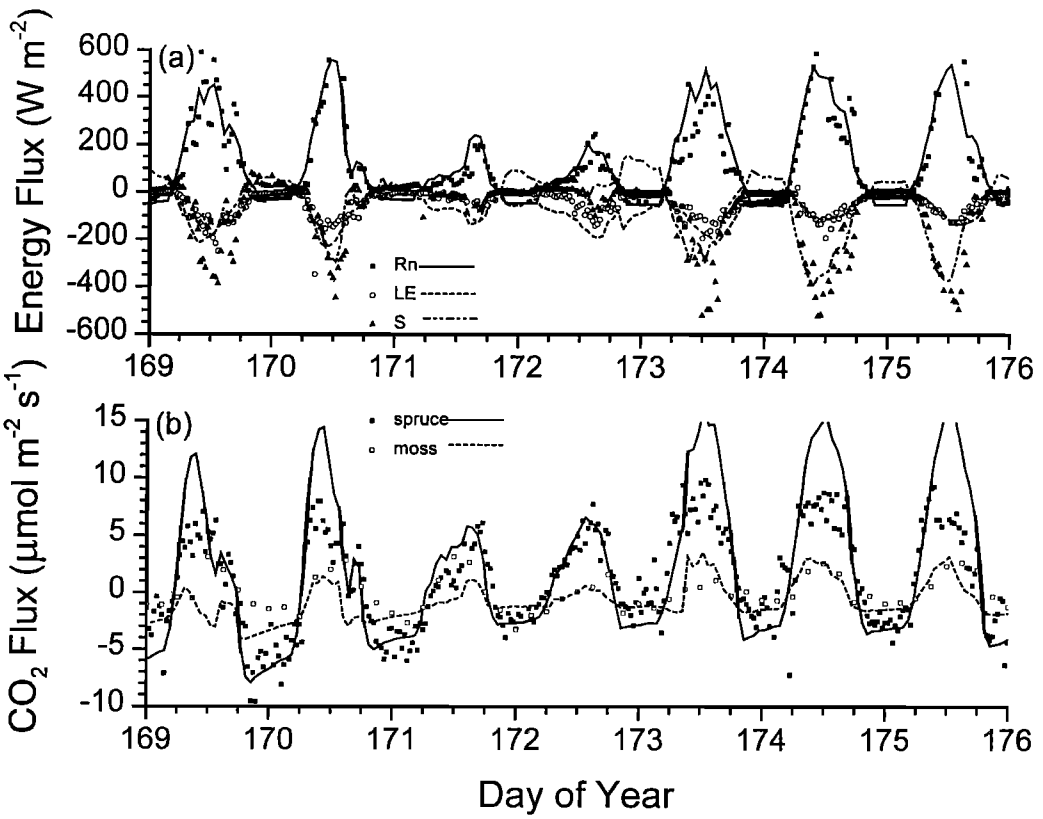

Figure 3. (a) Energy fluxes over black spruce and (b) CO_2 fluxes over black spruce and moss simulated (lines) and measured (symbols) at the northern old black spruce site from June 18 to 24 (DOY 170 to 176), 1996.

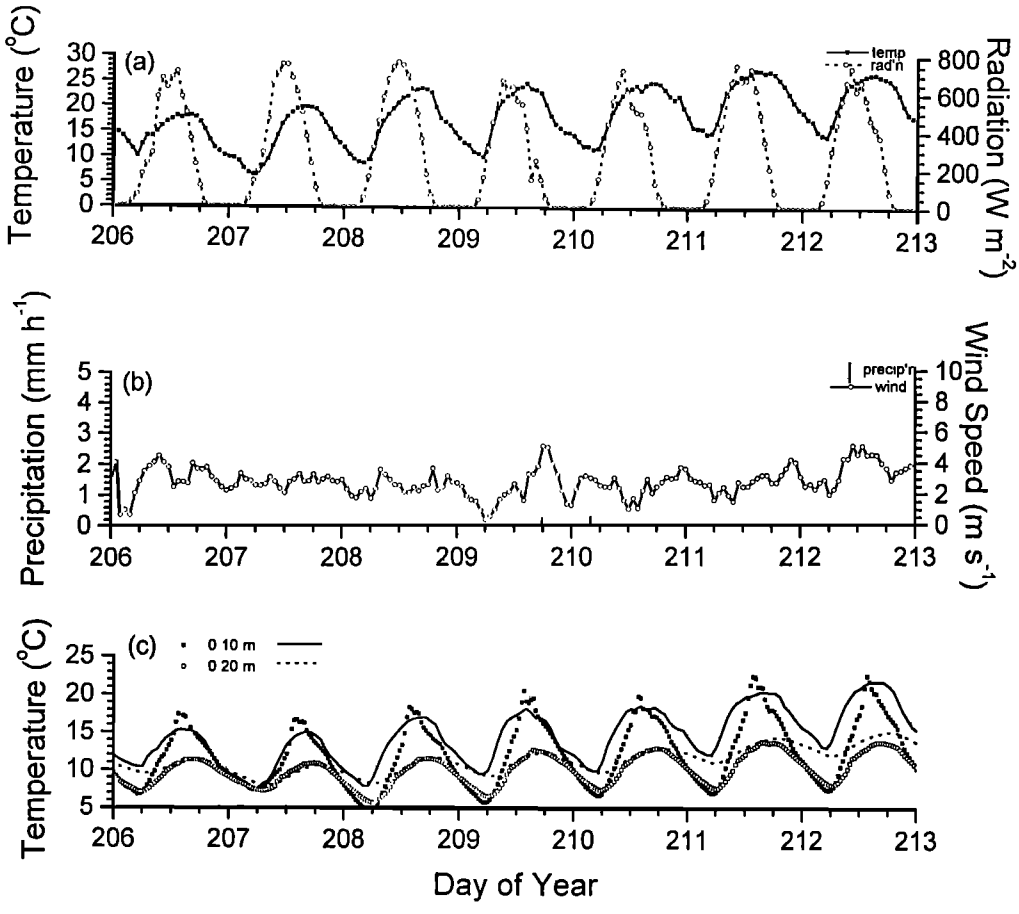

Figure 4. (a) Air temperature, radiation (b) precipitation, wind speed and (c) soil temperatures simulated (lines) and measured (symbols) at the northern old black spruce site from July 25 to 31 (DOY 207 to 213), 1996.

analysis of modeled versus measured daily NEP and evapotranspiration is given by *Amthor et al.* [this issue].

5.4. Annual C Exchange

Total ecosystem GPP modeled in 1994 of 803 g C m^{-2} (Table 3) was lower than that estimated from respiration chambers by *Ryan et al.* [1997] but was close to that estimated from eddy correlation fluxes by *Goulden et al.* [1997]. Spruce and moss GPP accounted for 624 g C m^{-2} (0.78) and 179 g C m^{-2} (0.22) respectively of this total. In comparison, *Goulden and Crill* [1997] estimated from flux measurements made with automated chambers and eddy correlation that moss accounted for 0.1 to 0.5 of total C fixation at this site. Autotrophic respiration in the model accounted for 0.64 and 0.60 of spruce and moss GPP respectively, leaving a total ecosystem NPP of 228 (spruce) + 71 (moss) = 299 g C m^{-2}. This NPP was larger than estimates of 219 and 252 g C m^{-2} by *Gower et al.* [1997, *Steele et al.* [1997] and *Ryan et al.* [1997] from allometry, litterfall, minirhizotrons and respiration flux chambers. These field estimates attributed only 10 g C m^{-2} of ecosystem NPP to moss, even though measurements of CO_2 fluxes by *Goulden and Crill* [1997] and of C storage by *Harden et al.* [1997] suggested that moss NPP was larger (e.g. Figs. 3b, 5b and 7b). Losses of C from senescence and root exudation in the model left a net biomass growth for spruce of 23 g C m^{-2} which was less than one of 78 g C m^{-2} estimated from allometric measurements by *Gower et al.* [1997], but consistent with growth rates of 20 g C m^{-2} yr^{-1} calculated by the *Alberta Forest Service* [1985] for black spruce trees of the climatic zone, age, height and diameter reported by *Gower et al.* [1997] from the old black spruce site.

Losses of 245 g C m^{-2} from heterotrophic respiration in the model left an annual NEP during 1994 of 54 g C m^{-2} (Table 3), of which 21 and 33 g C m^{-2} were attributed to gains in plant and soil C respectively. Weather during 1995 and 1996 was cooler and rainier than that during 1994 (average temperature and total precipitation in 1994, 1995 and 1996 were –2.07 °C, -2.55°C and –3.05°C, and 383 mm, 434 mm and 456 mm respectively). Cooler temperatures caused reductions in modeled GPP during 1995 and 1996 versus 1994 that were smaller than those in R_a + R_h, so that NEP rose to 67 and 60 g C m^{-2} in 1995 and 1996 from 54 g C m^{-2} in 1994. These changes in GPP and NEP with changes in climate follow from those modeled under short term changes in temperature (Figs. 3b, 5b and 7b). Gains in ecosystem C modeled during 1995 and 1996 were partitioned mostly to spruce wood. *Amthor et al.* [this issue] give a summary of the annual C and water balances estimated from eddy correlation fluxes measured between 1994 and 1996, and an analysis of the extent to which they corroborate model results.

After 150 years under the IS92a climate change scenario, C_a reached 1030 μmol mol^{-1}, maximum and minimum air temperatures had risen by 3.2°C and 4.4°C, and annual precipitation had risen by 65 mm. Higher C_a raised GPP in the model (Table 3) by raising CO_2 fixation rates (Figure 1b), and higher temperatures raised GPP further by extending the length

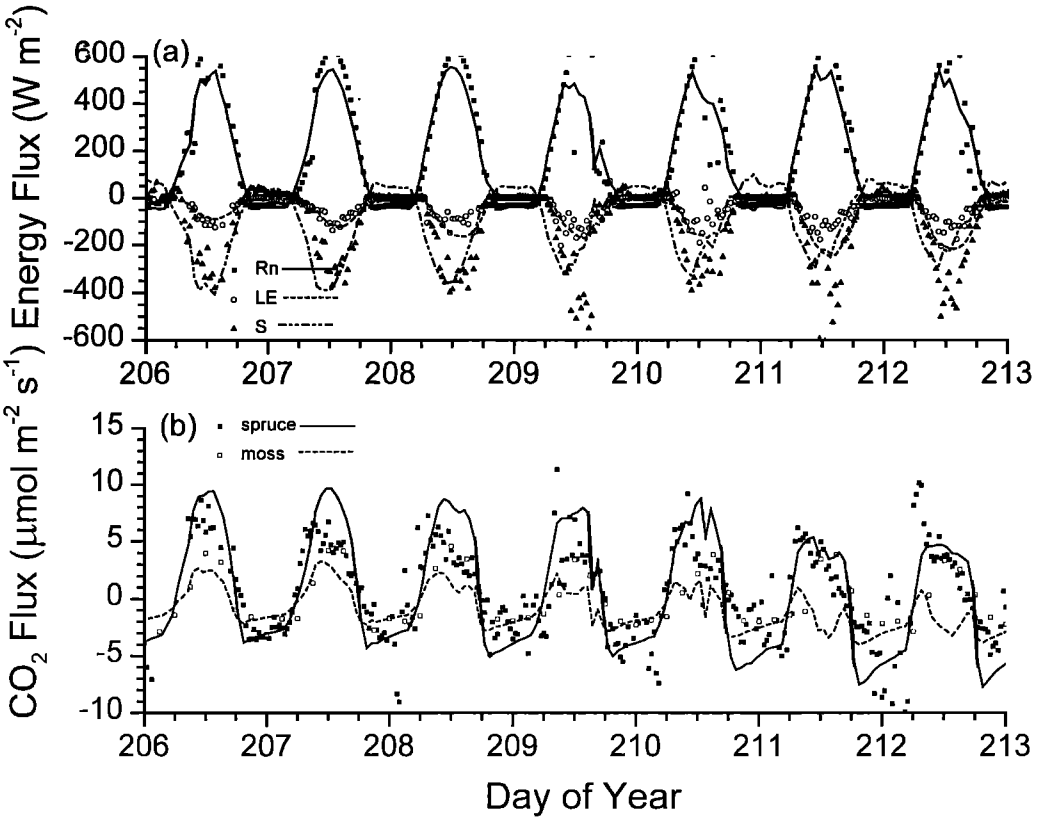

Figure 5. (a) Energy fluxes over black spruce and (b) CO_2 fluxes over black spruce and moss simulated (lines) and measured (symbols) at the northern old black spruce site from July 25 to 31 (DOY 207 to 213), 1996.

of the growing season within which CO_2 fixation occurred. However the rise in GPP was constrained in the model by N availability that caused foliar biomass and N concentrations to be reduced from current values. Higher air temperatures increased R_a comparatively more than GPP (e.g. Figure 5b) so that NPP rose only marginally from current values. Higher air temperatures caused higher soil temperatures with a longer period and greater depth of topsoil thawing, which increased R_h during the first 75 years of climate change. However after 150 years of climate change declining foliar biomass and N concentrations in the model caused lower soil C and N inputs that limited R_h. The modeled rise in NEP under climate change (112 versus 60 g C m^{-2} yr^{-1}) was entirely attributed to more rapid spruce growth (125 versus 46 g C m^{-2} yr^{-1}). This rise was partly an artifact of modeled spruce senescence, which sometimes alternated between lower and higher values during successive years so that annual rises in spruce growth under climate change alternated about a longer term mean. Climate change caused the soil to become a net C source (-10 g C m^{-2} yr^{-1}).

5.5. Long-Term C Accumulation

Annual values of NEP in the model (e.g. Table 3) were influenced by antecedent C stored in the spruce, moss and forest floor as affected by antecedent climate through its different effects on GPP, R_a and hence litterfall. More definitive estimates of annual NEP in this forest should therefore be derived from values simulated over several years. When run over a 150 year period, the model indicated very slow wood C accumulation during the first 75 years after seeding because N and P were sequestered by C turnover in moss (Figure 9a) which developed a C:N ratio of about 30. After 75 years the modeled spruce fully shaded the moss, reducing moss C turnover and N and P sequestration, so that more N and P became available for spruce growth. Spruce wood C then accumulated at a stable rate of 42 g C m^{-2} yr^{-1}. Wood C accumulation in the model is close to that derived from allometric equations for wood growth of black spruce for the site productivity index (fair) indicated by the age and height of the spruce trees at the experimental site (Alberta Forest Service, 1985] (Figure 9a). Early accumulation in the model was strongly affected by the competitive environment for nutrient acquisition provided by the moss. Total C accumulation modeled in wood, foliage and living moss after 150 years (4237, 381 and 19 g C m^{-2}) was less than that measured by *Gower et al.* [1997] (4300, 500 and 60 g C m^{-2}), but rising.

Soil C declined during the first 50 years of the model run while most C turnover occurred through moss, and then accumulated at a rate of 15 g C m^{-2} yr^{-1} for the next 100 years as spruce became the dominant source of litterfall (Figure 9b). *Nakane et al.* [1997] estimated soil C accumulations of 3 to 13 g C m^{-2} yr^{-1} from measurements of litterfall and soil respiration between June 1994 and May 1995 at the southern old black spruce site. *Harden et al.* [1997] estimated a net soil sequestration rate of 10 to 30 g C m^{-2} yr^{-1} from soil C accumulation at the northern old black spruce site, although *Goulden et al.* [1998] estimated a net soil loss of 80 g C m^{-2} yr^{-1} from eddy correlation fluxes measured in 1994.

Climate change raised wood C accumulation in the model to double its value under current climate after 150 years (Figure 9a). Total wood C accumulation in the model was comparable to one of 8350 g C m^{-2} derived from allometric equations for wood

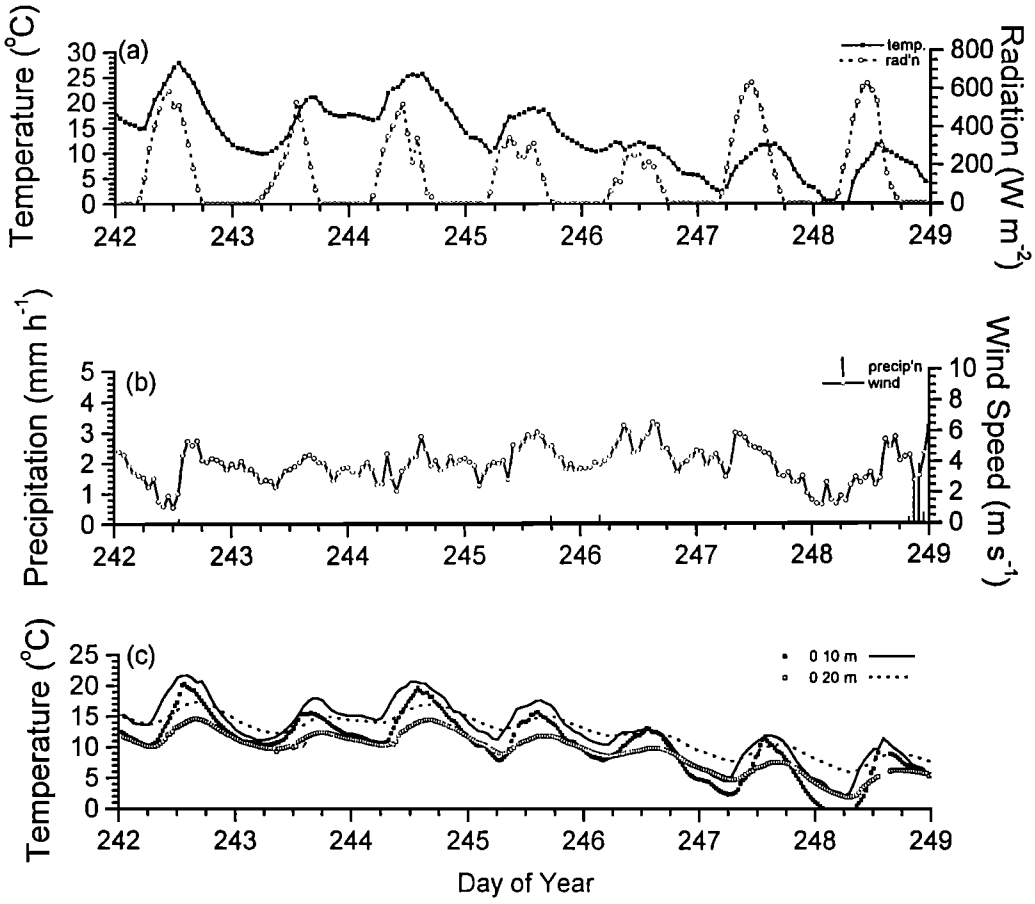

Figure 6. (a) Air temperature, radiation (b) precipitation, wind speed and (c) soil temperatures simulated (lines) and measured (symbols) at the northern old black spruce site from August 30 to September 5 (DOY 243 to 249), 1996.

growth of black spruce under current climate at a site with a good productivity index (the best index used by the *Alberta Forest Service*, 1985]. Soil C under climate change declined and recovered more rapidly than did that under current climate during the first 60 years of the model run (Figure 9b). However soil C did not continue to accumulate after 60 years under climate change, and started to decline after 130 years, whereas soil C accumulated steadily after 60 years under current climate.

6. Discussion

Mass and energy exchanges over black spruce forests are characterized by low CO_2 fixation rates and high Bowen ratios (Figs. 3a, 5a and 7a) even though these exchanges are not limited by soil water. These high ratios indicate a stomatal constraint to latent heat flux that might be caused by an environmental constraint to CO_2 fixation. Modeled CO_2 fixation in black spruce was strongly constrained by high stored C:N ratios in leaves that reduced the specific activities (Figure 1) and surface densities of leaf chlorophyll and rubisco to half of maximum values set from fertilization experiments (Table 1). These high C:N ratios occurred in the model because plant N uptake was limited by extremely low NH_4^+ and NO_3^- concentrations in the soil solution of the rooting zone. These low concentrations arose in the model from the slow mineralization of spruce detritus caused by their comparatively high lignin concentrations [*Trofymow et al* 1995] (Table 1), and from the slow mineralization of soil organic matter caused by its high soil C:N ratios (Table 2). Mineralization of plant detritus and soil organic matter was further slowed in the model by low specific microbial activity caused by low soil temperatures that developed under the large surface detritus (~400 g C m^{-2} in the model which was also measured at most of the black spruce sites sampled by Halliwell et al., 1995] that accumulated under the spruce and the moss. Reduced microbial activity was apparent in the low R_h modeled at the northern old black spruce site (245 g C m^{-2} yr^{-1} in Table 3). Low microbial activity in the model under spruce also resulted in low rates of N_2 fixation (ca. 0.5 g N m^{-2} yr^{-1} under spruce versus 2.5 g N m^{-2} yr^{-1} under aspen where modeled R_h = 525 g C m^{-2} yr^{-1} in *Grant et al.*, 1999a] that also contributed to low soil NH_4^+ and NO_3^- concentrations. These modeled fixation rates are within the ranges of 0.03 to 1.85 g N m^{-2} yr^{-1} and 0.35 to 3.25 g N m^{-2} yr^{-1} measured in soils under black spruce and aspen respectively by *Brouzes et al.* [1969]. Furthermore low pH (Table 1) reduced soluble P concentrations in the model [*Grant and Heaney*, 1997] and hence P uptake, growth and activity by both microbial and plant populations (notably moss, which developed roots only within the low pH zone in the upper 0.15 m of the soil profile).

Low CO_2 fixation rates caused by high C:N ratios forced low stomatal conductances in the model, based on the assumed conservation of the C_i:C_a ratio. Low conductances in black spruce (typically 0.02 – 0.04 mol CO_2 m^{-2} s^{-1} under full sunlight) were inferred from leaf chamber and C isotope

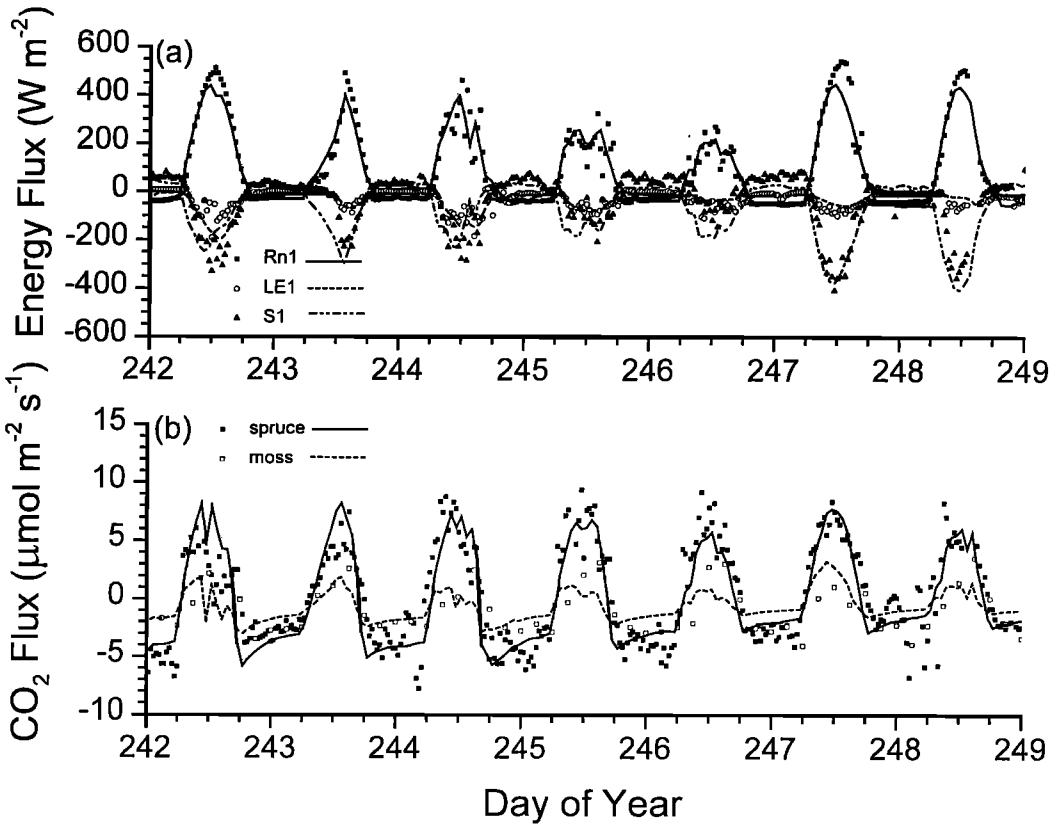

Figure 7. (a) Energy fluxes over black spruce and (b) CO_2 fluxes over black spruce and moss simulated (lines) and measured (symbols) at the northern old black spruce site from August 30 to September 5 (DOY 243 to 249), 1996.

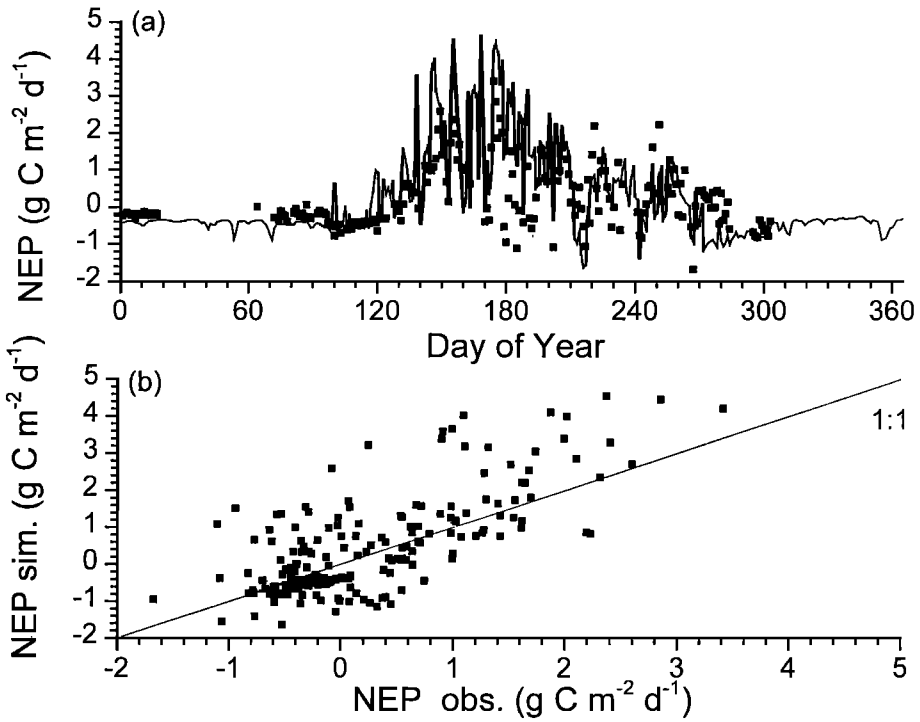

Figure 8. (a) Daily net ecosystem productivity (NEP) simulated (line) and measured (symbols), and (b) simulated versus observed NEP at the northern old black spruce site during 1996.

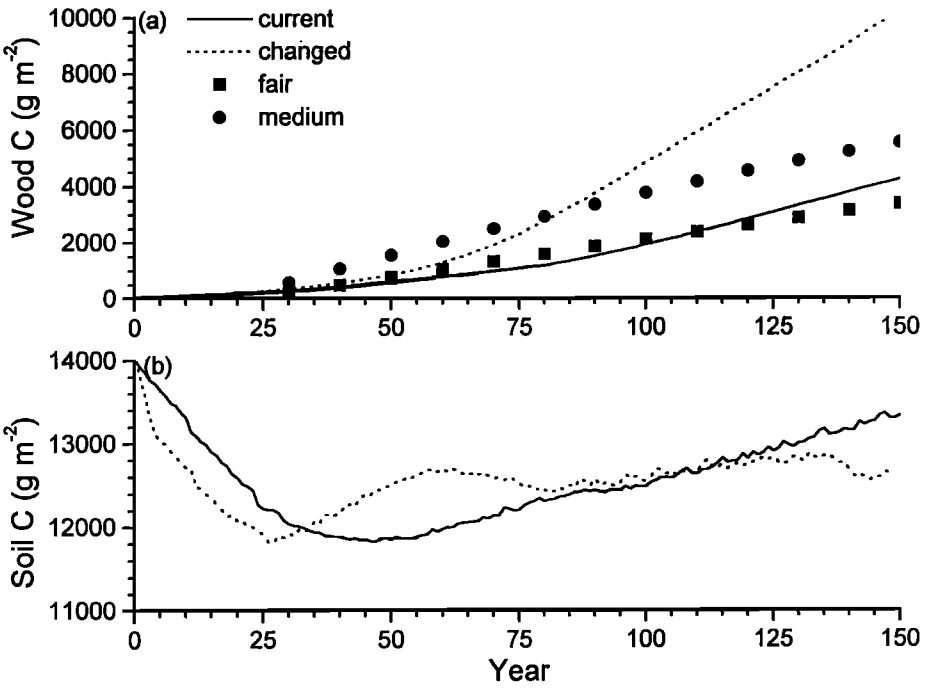

Figure 9. (a) Spruce wood C and (b) soil organic C simulated at the northern old black spruce site during 150 years under current (1994 - 1996) and hypothesized climates (lines), and (a) spruce wood C at fair and medium sites calculated from wood volume measurements by the *Alberta Forest Service* [(1985] (symbols).

discrimination studies by *Flanagan et al.* [1997] and measured with a portable photosynthesis system by *Middleton et al.* [1997]. These low conductances caused the small latent heat fluxes and large sensible heat fluxes modeled in Figs. 3a, 5a and 7a. Because the response of CO_2 fixation (Figure 1a) to irradiance above 500 μmol m^{-2} s^{-1} was limited, increases in net radiation were mostly offset by increases in sensible heat flux. Such increases were apparent in the field data, and have also been reported from eddy correlation measurements at the southern old black spruce site by *Jarvis et al.* [1997] and *Pattey et al.* [1997].

Small latent heat fluxes in the model caused low rates of water uptake from the soil, leading to periodic saturation, runoff and discharge (about 100 mm yr^{-1}). Surface water accumulation and high soil water contents were observed at the old black spruce site during much of 1994 [*Peck et al.*, 1997]. Wet soil further slowed mineralization of plant detritus and soil organic matter in the model because consequent low soil O_2 concentrations occasionally reduced energy yields from microbial activity [*Grant*, 1998b; *Grant and Pattey*, 1999] (Table 2). Low soil temperatures and O_2 concentrations also strongly constrained root growth [*Grant*, 1993a] below 0.35 m in the model, limiting plant access to deeper soil nutrients. Poor soil drainage has been directly linked to low foliar N concentrations and low growth rates of black spruce in Canadian boreal forests [*Lieffers and Macdonald*, 1990].

The low soil nutrient content at the old black spruce site thus caused a series of self-reinforcing processes in *ecosys* (low nutrient and high lignin content in spruce detritus → slow detritus decomposition → slow nutrient mineralization and biological N fixation → surface detritus accumulation→ cold soil → slow nutrient mineralization and biological N fixation → slow nutrient uptake → low CO_2 fixation → low transpiration → wet soil → slow detritus decomposition → slow nutrient mineralization and biological N fixation ...) that caused NPP and NEP to stabilize at low values (Table 3; Figure 9) in comparison to deciduous ecosystems in the same climate [*Grant et al.*, 1999a]. Soil warming under the IS92a climate change scenario caused a series of changes in these processes (warmer soil → faster detritus decomposition → faster nutrient mineralization and biological N fixation → slower surface detritus accumulation→ warmer soil → faster nutrient mineralization and biological N fixation → faster nutrient uptake → higher CO_2 fixation → faster detritus deposition → faster detritus decomposition → faster nutrient mineralization and biological N fixation ...) that caused NPP and NEP to rise over time. These changes with soil warming under IS92a were magnified by the earlier and deeper descent of the thawing front modeled during June and July.

The modeled spruce/moss forest remained a stable net sink for atmospheric C of about 40 (wood) + 15 (soil) = 55 g C m^{-2} yr^{-1} (Figure 9), largely because soil C oxidation was constrained in the model by the chemical composition of the detritus, and by the low nutrient, heat and periodically the low O_2 contents of the soil. The modeled soil C sink is consistent with that estimated by *Nakane et al.* [1997] and *Harden et al.* [1997]. The modeled wood C sink is consistent with a long-term average wood growth rate of 30 to 40 g C m^{-2} yr^{-1} estimated from aboveground measurements of ecosystem C at the northern old black spruce site by *Gower et al.* [1997]. It is also consistent with wood growth rates estimated by the *Alberta Forest Service* [1985] at fair to medium sites under climates comparable to that at the northern old black spruce site (Figure 9). These measured and modeled rates of soil and wood C accumulation suggest a NEP of 50 to 60 g C m^{-2} yr^{-1} by the black spruce/moss forest at this low-productivity site in the northern study area of BOREAS. This rate is less than that one of 100 (wood) + 30 (soil) g C m^{-2} yr^{-1}

simulated [*Grant et al.*, 1999a] and measured [*Black et al.*, 1996] at the southern old aspen site where rates of C cycling were larger. It is also less than the 60 (wood) + 10 (soil) g C m^{-2} yr^{-1} simulated [*Grant et al.*, 2001] and measured [*Jarvis et al.*, 1997] at the southern old black spruce site. Both these southern sites have mean annual temperatures ~2°C higher than that at the northern site simulated here. However if applied to the entire boreal forest zone, the NEP estimated at the northern old black spruce site would account for a global sink of 1 Gt C yr^{-1} [*Sellers et al.*, 1997]. Enhancement of this sink would require an improvement in the nutrient status of boreal black spruce forests, such as might occur if atmospheric N deposition rates were to rise. *Grant et al.* [2001] used *ecosys* to predict a substantial increase in wood C accumulation over 150 years by a black spruce stand in the southern study area of BOREAS under the IS92a climate change scenario should mineral N concentration in precipitation rise from 0.5 to 2.0 g N m^{-3}.

Rising C_a and air temperatures hypothesized under the IS92a climate change scenario are predicted by *ecosys* to cause a gain of 5000 g C m^{-2} by a boreal spruce-moss ecosystem after 150 years. However this gain would include a gain of 5700 g C m^{-2} in spruce wood and a loss of 700 g C m^{-2} in soil organic matter. These gains in wood C would be vulnerable to loss by fire and insects which are important natural disturbances in boreal ecosystems. The frequency of these disturbances may increase under a warmer climate, especially if increases in precipitation do not accompany those in temperature.

References

Alberta Forest Service, *Alberta Phase 3 Forest Inventory: Yield Tables for Unmanaged Stands,* Alberta Energy and Natl. Resour., Edmonton, Alberta, 1985.

Amthor, J.S., J.M. Chen, J. Clein, S. Frolking, M.L. Goulden, R.F. Grant, J.S. Kimball, A.W. King, A.D. McGuire, N.T. Nikolov, C.S. Potter, S. Wang, and S.C. Wofsy, Boreal forest CO_2 exchange and evapotranspiration predicted by nine ecosystem process models: inter-model comparisons and relationships to field measurements, *J. Geophys. Res.* this issue.

Berry, J.A., J. Collatz, J. Gamon, W. Fu, and A. Fredeen, BOREAS TE-04 Gas Exchange Data from Boreal Tree Species. http://www-eosdis.ornl.gov/ ORNL Distrib. Active Arch. Cent., Oak Ridge National Laboratory, Oak Ridge, Tennessee, 1998.

Betts, A.K., and J.H. Ball, Albedo over the boreal forest, *J. Geophys. Res., 102*, 28,901-28,909, 1997.

Black, T.A., et al., Annual cycles of water vapour and carbon dioxide fluxes in and above a boreal aspen forest, *Global Change Biol., 2*, 219-229, 1996.

Boer, G.J., N.A. McFarlane, and M. Lazare, Greenhouse gas-induced climate change simulated by the CCC second generation general circulation model. *J. Clim., 5*, 1045-1077, 1992.

Brouzes, R., J. Lasik, and R. Knowles, The effect of organic amendment, water content and oxygen on the incorporation of $^{15}N_2$ by some agricultural and forest soils, *Can. J. Microbiol. 15*, 899-905, 1969.

Chen, J.M., P.M. Rich, S.T. Gower, J.M. Norman, and S. Plummer, Leaf area index of boreal forests: Theory, techniques and measurements, *J. Geophys. Res., 102*, 29,429-29,443, 1997.

Ciais, P., P.P. Tans, J.W.C. White, M. Trolier, R.J. Francey, J.A. Berry, D.R. Randall, P.J. Sellers, J.G. Collatz, and D.S. Schimel, Partitioning of ocean and land uptake of CO_2 as inferred by $\delta^{13}C$ measurements from the NOAA Climate Monitoring and Diagnostic Laboratory Global Air Sampling Network, *J. Geophys. Res., 100*, 5051-5070, 1995.

Clymo, R.S., and P.M. Hayward, The ecology of *Sphagnum*, in *Bryophyte Ecology*, edited by A.J.E. Smith, pp. 229-289, Chapman and Hall, 1982.

Dang, Q.L., H.A. Margolis, M. Sy, M.R. Coyea, G.J. Collatz, and C.L. Walthall CL, Profiles of photosynthetically active radiation, nitrogen and photosynthetic capacity in the boreal forest: Implications for scaling from leaf to canopy. *J. Geophys. Res., 102*, 28,845-28,859, 1997.

Farquhar, G.D., S. von Caemmerer and J.A. Berry, A biochemical model of photosynthetic CO_2 assimilation in leaves of C_3 species, *Planta, 149*, 78-90, 1980.

Flanagan, L.B., J.R. Brooks, and J.R. Ehleringer, Photosynthesis and carbon isotope discrimination in boreal forest ecosystems: A comparison of functional characteristics in plants from three mature forest types, *J. Geophys. Res., 102*, 28,861-28,869, 1997.

Goulden, M.L., and P.M. Crill, Automated measurements of CO_2 exchange at the moss surface of a black spruce forest, *Tree Physiol., 17*, 537-542, 1997.

Goulden, M.L., B.C. Daube, S-M. Fan, D.J. Sutton, A. Bazzaz, J.W. Munger, and S.C. Wofsy, Physiological responses of a black spruce forest to weather. *J. Geophys. Res., 102*, 28,987-28,996. 1997.

Goulden, M.L., J.W. Munger, S-M. Fan, B.C. Daube, and S.C. Wofsy, Measurements of carbon sequestration by long-term eddy covariance: Methods and a critical evaluation of accuracy. *Global Change Biol.. 2*, 169-182, 1996.

Goulden, M.L., S.C. Wofsy, J.W. Harden, S.E. Trumbore, P.M. Crill, S.T. Gower, T. Fries, B.C. Daube, S-M. Fan, D.J. Sutton, A. Bazzaz, and J.W. Munger, Sensitivity of boreal forest carbon balance to soil thaw. *Science* 279, 214-217, 1998.

Gower, S.T., J.G. Vogel, J.M. Norman, C.J. Kucharik, S.J. Steele and T.K. Stow, Carbon distribution and aboveground net primary production in aspen, jack pine and black spruce stands in Saskatchewan and Manitoba, Canada, *J. Geophys. Res., 102*, 29,029-29,041, 1997

Grant, R.F., The distribution of water and nitrogen in the soil-crop system: A simulation study with validation from a winter wheat field trial, *Fert. Res., 27*,199-214, 1991.

Grant, R.F., Simulation of carbon dioxide and water deficit effects upon photosynthesis of soybean leaves with testing from growth chamber studies. *Crop Science 32*, 1313-1321, 1992a.

Grant, R.F., Simulation of carbon dioxide and water deficit effects upon photosynthesis and transpiration of soybean canopies with testing from growth chamber studies. *Crop Science 32*, 1322-1328, 1992b.

Grant RF (1993a) Simulation model of soil compaction and root Grant, R.F., Simulation model of soil compaction and root growth, I, Model development, *Plant Soil, 150*, 1-14, 1993a.

Grant, R.F., Simulation model of soil compaction and root growth, II, Model testing, *Plant Soil 150*, 15-24, 1993b.

Grant, R.F., Simulation of competition between barley (*Hordeum vulgare* L.) and wild oat (*Avena fatua* L.) under different managements and climates, *Ecol. Model., 71*, 269-287, 1994a.

Grant, R.F. Simulation of ecological controls on nitrification, *Soil Biol. Biochem. 26*, 305-315, 1994b.

Grant, R.F., Mathematical modelling of nitrous oxide evolution during nitrification, *Soil Biol. Biochem. 27*, 1117-1125, 1995.

Grant, R.F., *Ecosys*. in *Global Change and Terrestrial Ecosystems Focus 3 Wheat Network: Model and Experimental Meta. Data*, 2nd Ed., pp. 65-74, GCTE Focus 3 Office, NERC Centre for Ecol. and Hydrol., Wallingford, Oxon, U.K., 1996a.

Grant, R.F., *Ecosys*, in *Global Change and Terrestrial Ecosystems Task 3.3.1 Soil Organic Matter Network (SOMNET): 1996 Model and Experimental Metadata*, pp. 19-24, GCTE Focus 3 Office, NERC Centre for Ecol. and Hydrol., Wallingford, Oxon, U.K., 1996b.

Grant, R.F., Changes in soil organic matter under different tillage and rotation: Mathematical modelling in *ecosys*, *Soil Sci. Soc. Am. J., 61*, 1159-1174, 1997.

Grant, R.F., Simulation in *ecosys* of root growth response to contrasting soil water and nitrogen, *Ecol. Model., 107*, 237-264, 1998a.

Grant, R.F., Simulation of methanogenesis in the mathematical model *ecosys*, *Soil Biol. Biochem. 30*, 883-896, 1998b.

Grant, R.F., Simulation of methanotrophy in the mathematical model *ecosys*, *Soil Biol. Biochem., 31*, 287-297, 1999.

Grant, R.F., A review of the Canadian ecosystem model *ecosys*. Chap. 6 in *Modeling Carbon and Nitrogen Dynamics for Soil Management*, edited by Shaffer, M., CRC Press, Boca Raton, Fla., 2001.

Grant, R.F., and D.D. Baldocchi, Energy transfer over crop canopies: simulation and experimental verification, *Agric. For. Meteorol., 61*, 129-149, 1992.

Grant, R.F., and D.J. Heaney, Inorganic phosphorus transformation and transport in soils: mathematical modelling in *ecosys*, *Soil Sci. Soc. Am. J., 61*, 752-764, 1997.

Grant, R.F., and J.D. Hesketh, Canopy structure of maize (*Zea mays* L.) at different populations: Simulation and experimental verification, *Biotronics, 21*, 11-24, 1992.

Grant, R.F., and E. Pattey, Mathematical modelling of nitrous oxide emissions from an agricultural field during spring thaw, *Global Biogeochem. Cycles, 13*, 679-694, 1999.

Grant, R.F., and J.A. Robertson, Phosphorus uptake by root systems: mathematical modelling in *ecosys, Plant Soil, 188*, 279-297, 1997.

Grant, R.F., and P. Rochette, Soil microbial respiration at different temperatures and water potentials: Theory and mathematical modelling, *Soil Sci. Soc. Am. J., 58*, 1681-1690, 1994.

Grant, R.F., N.G. Juma, and W.B. McGill, Simulation of carbon and nitrogen transformations in soils. I. Mineralization, *Soil Biol. Biochem., 27*, 1317-1329, 1993a.

Grant, R.F., N.G. Juma, and W.B. McGill, Simulation of carbon and nitrogen transformations in soils. II. Microbial biomass and metabolic products, *Soil Biol. Biochem., 27*, 1331-1338, 1993b.

Grant, R.F., M. Nyborg, and J. Laidlaw, Evolution of nitrous oxide from soil: I. Model development, *Soil Sci., 156*, 259-265, 1993c.

Grant, R.F., M. Nyborg, and J. Laidlaw, Evolution of nitrous oxide from soil: II. Experimental results and model testing, *Soil Sci., 156*, 266-277, 1993d.

Grant, R.F., P. Rochette, and R.L. Desjardins, Energy exchange and water use efficiency of crops in the field: Validation of a simulation model, *Agron. J., 85*, 916-928, 1993e.

Grant, R.F., Garcia, R.L., Pinter Jr, P.J., Hunsaker, D., Wall, G.W., Kimball, B.A. and LaMorte, R.L., Interaction between atmospheric CO_2 concentration and water deficit on gas exchange and crop growth: Testing of *ecosys* with data from the Free Air CO_2 Enrichment (FACE) experiment. *Global Change Biol. 1*, 443-454, 1995a.

Grant, R.F., R.C. Izaurralde, and D.S. Chanasyk, Soil temperature under different surface managements: Testing a simulation model, *Agric. For. Meteorol. 73*, 89-113, 1995b.

Grant, R.F., B.A. Kimball, P.J. Pinter Jr., G.W. Wall, R.L. Garcia, and R.L. LaMorte, CO_2 effects on crop energy balance: Testing *ecosys* with a Free-Air CO_2 Enrichment (FACE) Experiment, *Agron. J., 87*, 446-457, 1995c.

Grant, R.F., R.C. Izaurralde, M. Nyborg, S.S. Malhi, E.D. Solberg and D. Jans-Hammermeister, Modelling tillage and surface detritus effects on soil C storage under current vs. elevated CO_2 and temperature in *ecosys*, in *Soil Processes and the Carbon Cycle*, edited by R. Lal et al., pp. 527-547, CRC Press. Boca Raton, Fla., 1998.

Grant, R.F., T.A. Black, G. den Hartog, J.A. Berry, H.H. Neumann, P.D. Blanken, P.C. Yang, C. Russell, and I.A. Nalder, Diurnal and annual exchanges of mass and energy between an aspen-hazelnut forest and the atmosphere: testing the mathematical model *ecosys* with data from the BOREAS experiment, *J. Geophys. Res., 104*, 27,699-27,717, 1999a.

Grant, R.F., G.W. Wall, K.F.A. Frumau, P.J. Pinter Jr., D. Hunsaker, B.A. Kimball, and R.L. LaMorte, Crop Water Relations under Different CO_2 and Irrigation: Testing of *ecosys* with the Free Air CO_2 Enrichment (FACE) Experiment, *Agric. For. Meteorol., 95*, 27-51, 1999b.

Grant, R.F., P.G. Jarvis, J.M. Massheder, S.E. Hale, J.B. Moncrieff, M. Rayment, S.L. Scott, and J.A. Berry, Controls on carbon and energy exchange by a black spruce – moss ecosystem: testing the mathematical model *ecosys* with data from the BOREAS experiment *Global Biogeochem. Cycles.* in press, 2001.

Halliwell, D.H., M.J. Apps, and D.T. Price, A survey of the forest site characteristics in a transect through the central Canadian boreal forest, *Water Soil Air Poll., 82*, 257-270, 1995.

Harden, J.W., K.P. O'Neill, S.E. Trumbore, H. Veldhuis, and B.J. Stocks, Moss and soil contributions to the annual net carbon flux of a maturing boreal forest, *J. Geophys. Res., 102*, 28,805-28,816, 1997.

Itoh, S., and S.A. Barber, Phosphorus uptake by six plant species as related to root hairs, *Agron. J., 75*, 457-461, 1983.

Jarvis, P.G., J.M. Massheder, S.E. Hale, J.B. Moncrieff, M. Rayment, and S.L. Scott, Seasonal variation in carbon dioxide, water vapor, and energy exchanges of a boreal black spruce forest, *J. Geophys. Res., 102*, 28,953-28,966, 1997.

Kaminsky, K.Z. and R. Dubayah, Estimation of surface net radiation in the boreai forest and northern prairie from shortwave flux measurements. *J. Geophys. Res., 102*, 29,707-27,716, 1997.

Kattenberg, A., F. Giorgi, H. Grassl, G.A. Meehl, J.F.B. Mitchell, R.J. Stouffer, T. Tokioka, A.J. Weaver, and T.M.L. Wigley, Climate models - Projection of future climate, in *Climate Change 1995*. edited by J.T. Houghton et al., pp. 285-357, Cambridge Univ. Press, New York, 1996.

Keeling, C.D., T.P. Whorff, M. Wahlen, and J. van der Piicht, Interannual extremes in the rate of rise of atmospheric carbon dioxide since 1980, *Nature, 375*, 666-670, 1995.

Lieffers, V.J. and S.E. Macdonald, Growth and nutrient status of black spruce and tamarack in relation to depth of water table

in some Alberta peatlands, *Can. J. For. Res., 20*, 805-809, 1990.

Mahendrappa, M.K. and P.O. Salonius, Nutrient dynamics and growth responses in a fertilized black spruce stand, *Soil Sci. Soc. Am. J., 46*, 127-133, 1982.

Makino, A., M. Harada, T. Sato, H. Nakano, and T. Mae, Growth and N allocation in rice plants under CO_2 enrichment. *Plant Physiol. 115*, 199-203, 1997.

Middleton, E.M., J.H. Sullivan, B.D. Bovard, A.J. Deluca, S.S. Chan and T.A. Cannon, Seasonal variability in foliar characteristics and physiology for boreal forest species at the five Saskatchewan tower sites during the 1994 Boreal Ecosystem-Atmosphere Study, *J. Geophys. Res., 102*, 28,831-28,844, 1997.

Mitchell, J.F.B., R.A. Davis, W.J. Ingram and C.A. Senior, On surface temperatures, greenhouse gasses and aerosols: models and observations. *J. Clim 10*, 2364-2386, 1995.

Mugasha, A.G., D.J. Pluth, K.O. Higginbotham, and S.K. Takyi, Foliar responses of black spruce to thinning and fertilization on a drained shallow peat, *Can. J. For. Res., 21*, 152-163, 1991.

Nakane, K., T. Kohno, T. Horikoshi, and T. Nakatsubo, Soil carbon cycling at a black spruce (*Picea mariana*) forest stand in Saskatchewan, Canada, *J. Geophys. Res., 102*, 28,785-28,793, 1997.

Pattey, E., R.L. Desjardins, and G. St-Amour, Mass and energy exchanges over a black spruce forest during key periods of BOREAS 1994, *J. Geophys. Res., 102*, 28,967-28,975, 1997.

Peck, E.L., T.R. Carroll, R. Maxson, B. Goodison, and J. Metcalfe, Variability of soil moisture near flux towers in the BOREAS southern study area, *J. Geophys. Res., 102*, 29,379-29,388, 1997.

Proctor, M.C.F., Physiological ecology: Water relations, light and temperature responses, carbon balance, in *Bryophyte Ecology*. edited by A.J.E. Smith, pp. 333-381, Chapman and Hall, 1982.

Ryan, M.G., M.B. Lavigne, and S.T. Gower, Annual cost of autotrophic respiration in boreal forest ecosystems in relation to species and climate, *J. Geophys. Res., 102*, 28,871-28,883, 1997.

Schubert, K.R. (Ed.), *The Energetics of Biological Nitrogen Fixation*, 30 pp., Am. Soc. Plant Physiol., Rockville, Md., 1982.

Sellers, P.J., F.G. Hall, and BOREAS members, BOREAS in 1997: Experiment review, scientific results, and future directions, *J. Geophys. Res., 102*, 28,731-28,769, 1997.

Shulten, H.-R., and M. Schnitzer, Chemical model structures for soil organic matter and soils, *Soil Sci., 162*, 115-130, 1997.

Steele, S.J., S.T. Gower, J.G. Vogel, and J.M. Norman, Root mass, net primary production and turnover in aspen, jack pine and black spruce forests in Saskatchewan and Manitoba, Canada, *Tree Physiol., 17*, 577-587, 1997.

Sutton, D., M. Goulden, and S. Wofsy, BOREAS TF-03 NSA-OBS tower flux, meteorological, and soil temperature data, http://www-eosdis.ornl.gov/] ORNL Distrib. Active Arch. Cent., Oak Ridge Nat. Lab., Oak Ridge, Tenn., 1998.

Thornley, J.H., Shoot:root allocation with respect to C, N and P: an investigation and comparison of resistance and teleonomic models, *Ann. Bot., 75*, 391-405, 1995.

Trofymo, J.A., C.M. Preston, and C.E. Prescott, Litter quality and its potential effect on decay rates of materials from Canadian forests, *Water Air Soil Poll., 82*, 215-226, 1995.

Troth, J.L., J. Deneke, and L.M. Brown, Upland aspen/birch and black spruce stands and their soil properties in interior Alaska, *For. Sci., 22*, 33-44, 1976.

Wofsy, S.C., M.L. Goulden, J.W. Munger, S-M. Fan, P.S. Bakwin, B.C. Daube, S.L. Bassow, and F.A. Bazzaz, Net exchange of CO_2 in a mid-latitude forest. *Science 260*, 1314-1317, 1993.

J A. Berry, Department of Plant Biology, Carnegie Institution of Washington, Stanford, CA 94305.

M. L. Goulden, Department of Earth System Science, University of California, Irvine, CA 92717.

R. G. Grant, Department of Renewable Resources, University of Alberta, Canada T6G 2E1. (robert.grant@ualberta.ca)

S. C. Wofsy, Department of Earth and Planetary Sciences, Harvard University, Cambridge, MA 02318.

(Received August 24, 2000; revised December 14, 2000;
accepted January 18, 2001.)